

1 **A Multiplex PCR Assay for Identifying All Major SARS-CoV-2 Variants**

2 **Short title: SARS-CoV-2 Variant Multiplex PCR Assay**

3 **Ryan J. Dikdan¹ BS, Salvatore AE Marras^{1,2} PhD, Amanda P. Field³ MPH, Alicia Brownlee³ BS, Alexander**
4 **Cironi³ BS, D. Ashley Hill³ MD, and Sanjay Tyagi^{1,4} PhD**

5 ¹Public Health Research Institute, New Jersey Medical School, Rutgers University, Newark, New Jersey

6 ²Department of Microbiology, Biochemistry and Molecular Biology, New Jersey Medical School, Rutgers
7 University, Newark, New Jersey

8 ³ResourcePath LLC, Sterling, VA

9 ⁴Department of Medicine, New Jersey Medical School, Rutgers University, Newark, New Jersey

L0 **Text Pages (not including title page, tables, or figure legends): 16 Tables: 1 Figures: 4**

L1 **Conflicts of Interest**

L2 Dr. D. Ashley Hill is the Medical Director of ResourcePath and Amanda P. Field, Alicia Brownlee, and Alex Cironi
L3 are employed by ResourcePath. ResourcePath partly funded this work through a grant to Rutgers. Ryan J.
L4 Dikdan, Salvatore A.E. Marras, and Sanjay Tyagi declare no conflicts of interests.

L5 **Support:** This research was supported through a grant from NIH R01 CA227291 and a grant from
L6 ResourcePath, LLC.

L7 **Correspondence:**

L8 rijd254@njms.rutgers.edu

L9 tyagisa@njms.rutgers.edu

L10 **Corresponding address for both: Public Health Research Institute, Rutgers University, ICPH Building Rm**
L11 **W310E, 225 Warren Street, Newark NJ 07103**

Abstract

Variants of Concern (VOC) of SARS-CoV-2, including Alpha, Beta, Gamma, and Delta, threaten to prolong the pandemic leading to more global morbidity and mortality. Genome sequencing is the mainstay of tracking the development and evolution of the virus, but is costly, slow, and not easily accessible. A multiplex qRT-PCR assay for SARS-CoV-2 was developed, which identifies all VOC as well as other mutations of interest in the viral genome, eight mutations total, using single nucleotide discriminating molecular beacons in a two-tube assay. The sensitivity and specificity of the assay was tested using *in vitro*-transcribed targets. Twenty-six SARS-CoV-2 positive patient samples were blinded, then tested using this assay and compared with deep sequencing results. The presented variant molecular beacon assay showed high accuracy when testing *in vitro*-transcribed targets, down to a limit of detection of five copies of the viral RNA, with 100% specificity. When testing patient samples, the assay was in full agreement with results from deep sequencing with a sensitivity and specificity of 100% (26/26). We have developed a qRT-PCR assay for the identification of currently circulating VOC of SARS-CoV-2 as well as other important mutations in its Spike protein coding sequence. This assay can be easily implemented on broadly available five-color thermal cyclers and will help track the spread of these variants.

37 Introduction

38 The COVID-19 pandemic has changed the world, leading to at least 4.6 million deaths and many permanent
39 injuries, with over 228 million cases worldwide as of 20 September 2021
40 (<https://www.who.int/emergencies/diseases/novel-coronavirus-2019>). Despite advances in diagnosis and
41 vaccination, the emergence of SARS-CoV-2 variants threatens to keep the pandemic going¹. The World Health
42 Organization and the US Centers for Disease Control (CDC)([https://www.cdc.gov/coronavirus/2019-
43 ncov/variants/variant-info.html](https://www.cdc.gov/coronavirus/2019-ncov/variants/variant-info.html)) have identified SARS-CoV-2 Variants of Concern (VOCs), which lead to
44 increased disease severity ([https://www.gov.uk/government/publications/nervtag-paper-on-covid-19-variant-
45 of-concern-b117](https://www.gov.uk/government/publications/nervtag-paper-on-covid-19-variant-of-concern-b117)), increased transmission², and immune/vaccine evasion³⁻⁵. Variants of Interest (VOIs) have
46 also been identified that present theoretical risks because they possess mutations similar to the mutations in
47 the VOC. Substitutions of Therapeutic Concern (STCs) have also been identified by the CDC which can affect
48 therapeutic antibody treatments for patients infected with such variants
49 (<https://www.fda.gov/media/145802/download>). These new variants and substitutions necessitate new tools
50 for their detection and tracking⁶.

51 Currently, the most common technique to identify, classify, and track variants of SARS-CoV-2 is deep
52 sequencing^{7,8}. While sequencing is accurate and can identify each mutation present in a sample, it is costly,
53 slow, and requires specialized instruments and interpretation when compared to other genotyping
54 techniques, such as Polymerase Chain Reaction (PCR)¹. Although, PCR assays target preselected mutations,
55 they are cheaper and more accessible than sequencing for the genotyping of SARS-CoV-2, and they yield faster
56 results. These methods may permit better tracking of variants as they spread throughout populations over
57 time, especially in resource limited settings¹.

58 Several SARS-CoV-2 variant genotyping PCR assays have been developed. They utilize TaqMan probes
59 (<https://www.thermofisher.com/us/en/home/clinical/clinical-genomics/pathogen-detection-solutions/real->

50 [time-pcr-research-solutions-sars-cov-2/mutation-panel.html](https://www.time-pcr-research-solutions-sars-cov-2/mutation-panel.html)), sloppy molecular beacon probes followed by
51 melting temperature analysis⁹, and several other strategies ([https://perkinelmer-](https://perkinelmer-appliedgenomics.com/home/sars-cov-2-testing-solutions/pkamp-variantdetect-sars-cov-2-rt-pcr-assay/)
52 [appliedgenomics.com/home/sars-cov-2-testing-solutions/pkamp-variantdetect-sars-cov-2-rt-pcr-assay/](https://perkinelmer-appliedgenomics.com/home/sars-cov-2-testing-solutions/pkamp-variantdetect-sars-cov-2-rt-pcr-assay/),
53 <https://info.biomeme.com/covid-19>, <https://www.aldatubio.com/product/pandaa-gdx-sars-covar>). However,
54 these assays either target single mutations per reaction or lack the appropriate number of targets to
55 thoroughly characterize SARS-CoV-2. Assays that detect multiple mutations at the same time are needed for
56 identification of circulating VOCs, VOIs, and for the identification of STCs.

57 Our approach is to create a multiplex assay for SARS-CoV-2 variants by exploiting the superior selectivity and
58 self-quenching characteristics of molecular beacons. Molecular beacons can be designed to selectively bind to
59 a mutant target sequence, while avoiding the wild-type sequence, which differs from the mutant by a single
60 nucleotide substitution. The interaction of a molecular beacon with its target is inherently more specific than
61 linear oligonucleotides that do not have a stem and loop structure, because target binding requires the
62 dissociation of the stem, which is thermodynamically costly¹⁰. The utility of this discriminatory power has been
63 previously demonstrated in real-time PCR for a number of applications^{11,12}.

64 Here we present a two-tube multiplex qRT-PCR assay that identifies current VOCs and VOIs by detecting eight
65 different mutations in the SARS-CoV-2 spike protein. We selected mutations that have been shown to increase
66 immune escape, avoid neutralization, and increase transmissibility. Targeting these causative mutations is
67 fruitful, because these strains may mutate and lose certain coincidental mutations, but mutations that
68 increase transmission and immune evasion are likely to be maintained. Also, by targeting these types of
69 mutations, it is possible to detect new variants that arise from combinations of previously confirmed
70 mutations. We also describe a molecular beacon design process that can be used to rapidly produce allele
71 discriminating assays for new variants as they arise.

72 **Materials and Methods**

33 **Synthetic RNA targets**

34 RNA standards of the SARS-CoV-2 whole genome and variant spike proteins were provided by Exact
35 Diagnostics through Bio-Rad Laboratories, Hercules, CA (catalog numbers COV019, COV019CE, COVA, COVB,
36 COVE, COVG).

37 An additional spike protein RNA sequence containing the E484Q and T478K mutations was generated from a
38 double-stranded synthetic DNA (gBlock) from Integrated DNA Technologies (Coralville, IA). A 5'-T7 promoter
39 was appended to it, which enabled transcription by T7 RNA polymerase, which was performed using the
30 HiScribe™ T7 High Yield RNA Synthesis Kit (New England Biolabs, Ipswich, MA). The RNA produced was purified
31 with a Monarch RNA Cleanup Kit, 50 µg, (New England Biolabs) and by denaturing polyacrylamide gel
32 electrophoresis, eluting the band of correct size in gel elution buffer (400 mM NaCl, 20 mM Tris-HCl (pH 8.0),
33 and 1 mM EDTA). The concentration of the eluted RNAs was determined by a NanoDrop spectrophotometer
34 (Thermo Fisher Scientific, Waltham, MA).

35 **Primer Design**

36 Primers were designed by using the primer3 server¹³. 200 nucleotides surrounding the mutation of interest on
37 either side of the SARS-CoV-2 genome was used as input, the target-binding region of the molecular beacon
38 was used as the hybridization probe, and the amplicon size was set between 50 to 300 nucleotides. The
39 sequences of all the primers that were used in the assay are shown in Table 1.

40 **Design and characterization of single nucleotide discriminating molecular beacons**

41 A key consideration in the design of single-nucleotide discriminating molecular beacons is that the melting
42 temperature (T_m) of the probe-target hybrid with the perfect target (in the present case, the mutant
43 sequence) is minimally above, only 3 to 7 °C, the annealing temperature of the PCR (which is the temperature
44 at which fluorescence will be monitored). This makes it so that the mismatched hybrid (in the present case,

the wild-type sequence) will not appreciably bind to the molecular beacon at the fluorescence monitoring temperature. Furthermore, the melting temperature of the stem of the molecular beacon should be above the detection temperature.

We designed our primers so that they will function at the PCR annealing temperature of 58 °C. We selected a region of sequence around the site of each mutation such that the T_m of the perfect probe-target hybrid was above the annealing temperature, but that the mismatched single-nucleotide polymorphism had a T_m lower than the annealing temperature. These T_m 's were predicted by using the DINAMelt¹⁴ two-state melting hybridization server with the following parameters: 0.25 μ M oligonucleotide concentration, $[Na^+] = 60$ mM, $[Mg^{2+}] = 3$ mM, for DNA at 58 °C.

After deciding upon the target binding region, a hairpin stem was created by appending 5 or 6 nucleotides on either side (with 4 to 5 G:C pairs) such that they are complementary to each other, but not complementary to the target. In addition, we ensured that the 5' nucleotide is not a guanosine, because that could lead to fluorescence quenching due to the 5' position of the fluorophore. These sequences were then ordered from either LGC Biosearch Technologies (Petaluma, CA) or from Eurofins (Luxembourg City, Luxembourg). They were purified by HPLC through a PRP-3 Reversed Phase HPLC Column (Hamilton Company, Reno, NV) in a Beckman System Gold HPLC System (Fullerton, CA). The desired fractions were then ethanol precipitated and resuspended in water, and their concentration was determined by NanoDrop spectrophotometer. The sequences of all molecular beacons that were used in the assay are shown in Table 1.

To determine if the designed sequences could sufficiently discriminate the alleles at the annealing temperature of the PCR assay, we measured the fluorescence of the molecular beacons in the presence of either a mutant target, a wild-type target or, no target, under the buffer conditions that are expected to be present during PCR. Each 25 μ L thermal denaturation reaction contained 20 mM Tris-HCl (pH 8.4), 50 mM KCl, 1.5 mM $MgCl_2$, 1 μ M oligonucleotide target, and 0.4 μ M molecular beacon. The fluorescence intensity of each

28 reaction was measured at every degree in the appropriate fluorescence channel as the temperature was
29 lowered from 95 °C to 30 °C (decreasing 1 °C/10 seconds) in a Bio-Rad CFX96 Touch Real-Time PCR Detection
30 System.

31 Melt curve signals were normalized, for each molecular beacon. The difference between a normalization point
32 and the other melt curve fluorescent signals was subtracted from the raw fluorescent intensity values and
33 then all values in that channel were divided by the maximum intensity for that molecular beacon, to derive
34 relative fluorescence units, which range between 0 and 1.

35 **Optimizing the concentrations of the qRT-PCR multiplex primers and molecular beacons**

36 qRT-PCR was performed with TaqMan Fast Virus 1-Step Master Mix (No ROX) to optimize conditions, and
37 TaqPath™ 1-Step Multiplex Master Mix (No ROX) (both from Applied Biosystems, Waltham, MA) for final
38 experiments and patient samples.

39 Asymmetric PCR was performed for each amplicon, where the primer generating the strand complementary to
40 the molecular beacon (labeled reverse) was in 5-fold excess over the other primer (labeled forward). All
41 molecular beacons were designed in the same forward strand direction. G:T mismatches can be discriminated
42 from each other by switching the strand being interrogated to the complementary strand¹⁵. The molecular
43 beacon and primer concentrations were adjusted by trial and error, for sufficient amplification and signal. The
44 final working concentrations of each of the components for each tube are listed in Table 1 along with their
45 sequences.

46 Each reaction had a final volume of 20 µL comprised of TaqPath or TaqMan Master 1-Step Mix (No ROX),
47 water, and primers and probes as previously described. 15 µL of this complete master mix was pipetted into
48 each PCR tube, and then 5 µL of sample was added and mixed, before running on the thermal cycler.

49 **Assay sensitivity and specificity**

50 The sensitivity of the assay was determined by preparing dilution series of *in vitro* transcribed targets (shown
51 vertically in Figure 3A), which were diluted 10-fold from 1,000 copies/ μ L to 0.1 copies/ μ L. 5 μ L of each of these
52 dilutions were combined with 15 μ L of completed master mix per reaction. The tubes were sealed, briefly
53 shaken, spun down at 800 g for 1 min. and then run on a Bio-Rad CFX96 Touch Real-Time PCR Detection
54 System with the TaqPath or TaqMan Fast specified thermal cycler conditions, and with an annealing
55 temperature of 58 °C. Specificity of the assay was determined by comparing the known sequences of the *in*
56 *vitro* transcribed targets with the signals in these dilution series. For patient samples, sensitivity and specificity
57 were determined by comparing this assay's results to sequencing results, which are the gold standard.

58 **Collection of patient samples and sequencing**

59 Patient mid-nasal swabs were collected for clinical testing in 1 ml of DNA/RNA Shield Reagent (Zymo, Irvine,
60 CA). 400 μ L aliquots were used for RNA extraction using the Kingfisher Flex magnetic bead extraction system
61 (Thermo Fisher Scientific) and the Zymo Quick RNA/DNA Magbead kit (Zymo) per manufacturer's instructions.
62 qRT-PCR screening was performed using 2 μ L of purified RNA, TaqPath 1-step Multiplex Master Mix (No ROX)
63 and an in-house validated multiplex assay. This screening assay, outlined in Figure S2, detects conserved
64 sequences in the N and RdRp genes of SARS-CoV-2, along with human β -actin mRNA, with high sensitivity. The
65 primers and molecular beacons targeting regions in the RdRp, N, and human β -actin genes were adapted from
66 previously validated assays ([https://www.cdc.gov/coronavirus/2019-ncov/lab/rt-pcr-panel-primer-](https://www.cdc.gov/coronavirus/2019-ncov/lab/rt-pcr-panel-primer-probes.html)
67 [probes.html](https://www.cdc.gov/coronavirus/2019-ncov/lab/rt-pcr-panel-primer-probes.html)), and are listed in Table S1. Samples were run on a Quantstudio 7 (Thermo Fisher Scientific).
68 Amplicon sequencing was performed using the Ion AmpliSeq SARS-CoV-2 Insight Research Panel (Ion Torrent,
69 Guilford, CT). Each library contained six samples, one positive control sample and one no template control.
70 Barcoded libraries were prepared using the Ampliseq Kit for Chef DL8 and Ion 530 Kit-Chef (Ion Torrent).
71 Sixteen libraries were combined to run on a single Ion 530 chip. Templates were prepared using the Ion 530
72 Chef Reagents template kit. Sequencing was performed on the Ion S5XL instrument with Ion S5 Sequencing

73 Solutions and Reagents (Ion Torrent). Sequence data was analyzed for on-target and mean depth of coverage
74 using the SARS_COV_2_Coverage Analysis plug-in v1.3.0.2 (Ion Torrent). FASTA files were created using the
75 IRMA report plug-in v1.3.0.2 (Ion Torrent). Sequence data and corresponding metadata were uploaded to
76 GISAID and are included as supplementary data. Aliquots of purified RNA samples no longer needed for
77 diagnosis were deidentified and transferred to Rutgers's laboratory for initial testing of the multiplex variant
78 molecular beacon assay.

79 **Multiplex qRT-PCR with patient samples**

30 Patient samples were tested in a similar manner to how we tested the assay's sensitivity and specificity. 5 μ L
31 of each sample was combined with 15 μ L each completed master mix using TaqPath and run as mentioned
32 before.

33 **qRT-PCR analysis and plotting**

34 Data generated from the CFX96 Touch Real-Time PCR Detection System was analyzed with Bio-Rad's CFX
35 Maestro Software Version 2.0, which corrects for fluorescence drift, subtracts the baseline, and fits curves to
36 each qRT-PCR signal. Threshold cycles (C_t) were determined via a manually specified single threshold of our
37 analyzed data, which was clearly above all negative control signals.

38 For the specificity plots in Figure 3A, fluorescent signals were normalized by dividing all values by the highest
39 fluorescent value in each channel for the respective tubes.

30 **Results**

31 **Design of a two-tube, eight mutation, multiplex qRT-PCR assay for SARS-CoV-2 Variants**

32 In our assay, SARS-CoV-2 variants were identified by probing the coding region of the spike protein transcript
33 for the presence of eight different point mutations, as detailed in Figure 1. Since only the mutants are

94 expected to yield a positive signal, we included an additional set of primers and molecular beacons for a
95 conserved region of the viral N gene in Tube one as a positive control for the presence of the virus. Since the
96 multiplexing capacity of common thermal cyclers is 4 or 5 colors, we divided the assay into two tubes. The
97 colors of the molecular beacons and the locations of the primers are indicated in Figure 1A. In Tube one,
98 there were three amplicons, and in Tube two, all four targets were present in the same amplicon.

99 Even though individual isolates of each variant may possess other mutations, we focused on sets of mutations
100 that are functionally the most important. By using *in vitro* binding and epidemiological data of how these
101 mutations affect immune evasion and binding to the ACE2 receptor^{2-5,17,18}, we chose to identify the mutations
102 shown in Figure 1: d69-70, K417N/T, L452R, T478K, E484K/Q, and N501Y. We also chose these mutations such
103 that a single mutation in Tube one is sufficient to identify most Variants of Concern (VOCs), which of course is
104 subject to change as the virus evolves. The mutations targeted in Tube two complete the identification of the
105 VOCs and identify the Substitutions of Therapeutic Concern (STCs) (<https://www.cdc.gov/coronavirus/2019-ncov/variants/variant-info.html>).

107 **The variant molecular beacon assay is specific for the identification of common SARS-CoV-2 variant** 108 **mutations**

109 Before assembling our multiplex assay, we designed molecular beacons for each targeted mutation,
110 determined their thermal denaturation profiles, and tested them in monoplex PCRs. To determine whether
111 the molecular beacons were allele discriminating at the annealing temperature, we determined the thermal
112 denaturation profiles of the molecular beacons by themselves, and together with mutant or wild-type targets.
113 In these experiments, the targets were synthetic oligonucleotides, and they were used in a molar excess above
114 the molecular beacon concentration. A representative profile is shown in Figure 2, and the profiles of all the
115 molecular beacons are shown in Supplementary Figure 1. Although, the window of discrimination varies
116 somewhat from molecular beacon to molecular beacon (Figure S1), all of our molecular beacons permitted

17 single nucleotide discrimination (see Figure 3A). After qualifying the molecular beacons in this manner, we
18 performed a set of monoplex PCR assays for each mutation, using wild-type targets and mutant targets in
19 alternate reactions.

20 When all the monoplex reactions indicated successful amplification and allele discrimination, we assembled two
21 multiplex reactions that included all the primers and molecular beacons, as detailed in Figure 1. To demonstrate
22 the specificity of the multiplex assays, six pairs of reactions were carried out, in which each reaction received
23 5,000 copies of either the wild type, B.1.1.7 (Alpha), B.1.351 (Beta), P.1 (Gamma), B.1.427 (Epsilon), or E484Q
24 and T478K (Kappa/Delta)-containing spike RNA sequences. The targets were *in vitro*-transcribed RNAs
25 corresponding to a portion of the spike protein, or commercially available RNA standards, as detailed in
26 methods and in the legend to Figure 3. The results of these reactions are presented in Figure 3A, where the
27 targets are indicated inside the panels, and the color response of each molecular beacon is indicated by the
28 color of the line. This data shows that when the wild-type SARS-CoV-2 genome is present, only the N gene
29 positive control signal occurs. When testing spike RNAs containing the variant mutations, the correct mutations
30 were identified. For example, the Beta variant (B.1.351) contains not only the uniquely identifying K417N
31 mutation, but also the N501Y and E484K mutation.

32 **The variant molecular beacon assay can detect at as few as five copies of viral RNA**

33 To demonstrate the sensitivity of the variant molecular beacon assay, PCR assays were initiated with serial
34 dilutions of each target. The results are shown in Figure 3B. Each dilution series tested from 5,000 copies to
35 0.5 copies. Where a clear signal was present, the threshold cycle was determined by a manually identified
36 single threshold for each channel. Reactions starting with as little as five copies yielded a detectable signal in
37 each case. The correlation coefficients between the logarithm of the copy number and the threshold cycles in
38 each case are each greater than 0.98, showing a very strong exponential relationship between the two. These

39 results also indicate that in Tube one, which contains four pairs of primers, the amplification of multiple
40 different amplicons does not interfere with each other, which would diminish sensitivity.

41 **Patient samples of varying strains of SARS-CoV-2 are accurately identified**

42 After demonstrating the specificity and sensitivity of the variant molecular beacon assay with *in vitro*-
43 transcribed RNAs, we performed this assay on a set of patient samples (RNA extracted from mid-nasal swabs)
44 that were SARS-CoV-2 positive, as identified by a molecular beacon screening assay, which we previously
45 developed. After being identified as positive for SARS-CoV-2 by this assay, the samples were sequenced to
46 identify all mutations present in the strains' genomes. Afterwards, the RNA extracted from the samples were
47 then provided to Rutgers in a blinded manner for variant identification.

48 These RNA samples were tested using the two-tube variant molecular beacon assay, as described above.
49 Figure 4 shows the threshold cycles for each molecular beacon target in each sample. All samples tested
50 positive for the N gene positive control signal. Two samples were identified as the Alpha variant (B.1.1.7 with
51 d69-70 and N501Y), two samples were identified as the Epsilon variant (B.1.427/429 with only L452R), eight
52 samples were identified as the Delta variant (B.1.617.2 with L452R and T478K), ten samples had the E484K
53 mutation, although not associated with any VOCs, and four samples had none of the targeted mutations and
54 therefore are not any of the currently identified VOCs or VOIs.

55 After strain identification was performed with the variant molecular beacon assay, the results were compared
56 with sequencing data (supplementary data), which was in complete agreement. Our results indicate 100%
57 sensitivity and specificity of the assay as tested so far. It is also notable that one of the samples possessed an
58 L452Q mutation, which is similar to the L452R mutation, but the L452R molecular beacon did not show a
59 fluorescent signal due to the L452Q mutation, further confirming the specificity of the results of our single
60 nucleotide discriminating molecular beacons.

51 Discussion

52 Molecular beacons designed to differentiate point mutations are an ideal tool for genotyping on a global scale
53 due to their ease of design and production. In the case of newer emerging variants, molecular beacons can
54 quickly be synthesized and validated for that variant's identification, which can help to monitor strains, and
55 improve patient care via epidemiological tracking. Utilizing the outlined strategy, molecular beacons for new
56 targets can be designed and added to the assay in two or three weeks. This assay not only enables the
57 identification of the four variants of concern and many variants of interest, but since it targets many known
58 mutations that confer increased transmission and immune evasion, it will be able to identify new variants that
59 recombine with existing mutations. An example of the assay's ability to pick up newer variants lies in the
60 newer Delta variant's mutations, which include the L452R mutation, which is also present in the Epsilon
61 variant.

62 Due to the specificity of the molecular beacons, similar mutations in the target region will not elicit false-
63 positive signals. Evidence of this is found in the lack of signal in one of the samples which contained the L452Q
64 mutation, as identified by sequencing. More evidence of the specificity is in the clean differentiation of the
65 K417T and K417N mutations, as well as the E484Q and E484K mutations. This specificity enables precise
66 identification, but also comes with the downside that mutations in the binding region of the molecular beacon
67 could result in false-negative signals, although no mutations like these were found in the samples that were
68 tested. Despite this, if other mutations do arise near the uniquely identifiable mutations, this can be
69 accounted for by either designing different molecular beacons, or by introducing degenerate nucleotides into
70 the current molecular beacons.

71 This study is limited by the number of patient samples tested. Accuracy in the presence of other

72 This assay introduces the sequences of many useful molecular beacons for the identification of point

73 mutations in SARS-CoV-2. This variant molecular beacon assay is most useful as a screening tool for positive

34 SARS-CoV-2 patient samples which can identify all major VOC and VOI (see Figure 1B and Table S2). The
35 primers and molecular beacons can also be combined in varying combinations to test for other pathogens,
36 they can be added to current assays, and they can be used with human RNA controls as were added in the
37 multiplex COVID-19 molecular beacon screening assay (see Supplementary Figure S2). These assays can then
38 be used to test for the most common variants in a region or to directly test human samples as a single
39 pathogen/COVID-19 variant identification test in general practice.

30 Here we describe a multiplexed molecular beacon assay for the classification of SARS-CoV-2 variants via their
31 identifying functional mutations. We have shown that the assay clearly differentiates between the different
32 SARS-CoV-2 variant sequences, and accurately classifies patient samples that have been identified by deep
33 sequencing technologies. All primer and probe sequences used in this assay are listed in Table 1 to facilitate
34 SARS-CoV-2 variant genotyping on a larger scale, and to address the public need for variant tracking.

35 **Acknowledgements**

36 This research was supported through a grant from NIH R01 CA227291 and a grant from ResourcePath, LLC. We
37 would like to specifically acknowledge Diana Y. Vargas for her help in designing the SARS-CoV-2 molecular
38 beacon screening assay.

39 **Conflicts of Interest**

30 Dr. D. Ashley Hill is the Medical Director of ResourcePath and Amanda P. Field, Alicia Brownlee, and Alex Cironi
31 are employed by ResourcePath. ResourcePath partly funded this work through a grant to Rutgers. Ryan J.
32 Dikdan, Salvatore A.E. Marras, and Sanjay Tyagi declare no conflicts of interests.

33 **Ethics Statement**

34 This study used archived, de-identified samples left over from clinical testing. The study received expedited approval
35 with full waiver of consent, Advarra IRB# Pro00058476.

06 **Data Sharing**

07 All sequencing data is available online through Mendeley Data at

08 <https://data.mendeley.com/datasets/v3n2dzt8st/1> .

09 **Authors' Contributions**

L0 Conceptualization and methodology were performed by RJD, SAEM, and ST. AH, AB, AC, AF provided the
L1 patient samples which were tested, and the sequencing results they generated were used to validate the
L2 assay used. The original draft was written by RJD, and review and editing were performed by all authors. ST
L3 and SAEM supervised RJD in running experiments.

L4 **References**

- L5 1. Fontanet A, Autran B, Lina B, Kieny MP, Karim SSA, Sridhar D. SARS-CoV-2 variants and ending the
L6 COVID-19 pandemic. *Lancet*, 2021, 397:952–4
- L7 2. Davies NG, Barnard RC, Jarvis CI, Kucharski AJ, Munday J, Pearson CAB, Russell TW, Tully DC, Abbott S,
L8 Gimma A, Waites W, Wong KLM, van Zandvoort K, Eggo RM, Funk S, Jit M, Atkins KE, Edmunds WJ,
L9 Houben R, Meakin SR, Quilty BJ, Liu Y, Flasche S, Lei J, Sun FY, Krauer F, Lowe R, Bosse NI, Nightingale
20 ES, Sherratt K, Abbas K, O'Reilly K, Gibbs HP, Villabona-Arenas CJ, Waterlow NR, et al. Estimated
21 transmissibility and severity of novel SARS-CoV-2 Variant of Concern 202012/01 in England. *MedRxiv*,
22 2020. <https://doi.org/10.1101/2020.12.24.20248822>
- 23 3. Deng X, Garcia-Knight MA, Khalid MM, Servellita V, Wang C, Morris MK, Sotomayor-González A, Glasner
24 DR, Reyes KR, Gliwa AS, Reddy NP, Sanchez San Martin C, Federman S, Cheng J, Balcerek J, Taylor J,
25 Streithorst JA, Miller S, Kumar GR, Sreekumar B, Chen P-Y, Schulze-Gahmen U, Taha TY, Hayashi J,
26 Simoneau CR, McMahon S, Lidsky P V, Xiao Y, Hemarajata P, Green NM, Espinosa A, Kath C, Haw M, Bell
27 J, Hacker JK, et al. Transmission, infectivity, and antibody neutralization of an emerging SARS-CoV-2

28 variant in California carrying a L452R spike protein mutation. MedRxiv Prepr Serv Heal Sci, 2021.

29 <https://doi.org/10.1101/2021.03.07.21252647>

- 30 4. Wang P, Casner RG, Nair MS, Wang M, Yu J, Cerutti G, Liu L, Kwong PD, Huang Y, Shapiro L, Ho DD.
31 Increased resistance of SARS-CoV-2 variant P.1 to antibody neutralization. Cell Host Microbe, 2021,
32 29:747-751.e4
- 33 5. Weisblum Y, Schmidt F, Zhang F, DaSilva J, Poston D, Lorenzi JCC, Muecksch F, Rutkowska M, Hoffmann
34 HH, Michailidis E, Gaebler C, Agudelo M, Cho A, Wang Z, Gazumyan A, Cipolla M, Luchsinger L, Hillyer
35 CD, Caskey M, Robbiani DF, Rice CM, Nussenzweig MC, Hatziioannou T, Bieniasz PD. Escape from
36 neutralizing antibodies 1 by SARS-CoV-2 spike protein variants. Elife, 2020, 9:1
- 37 6. Bandy DJDR, Weimer BC. Analysis of SARS-CoV-2 genomic epidemiology reveals disease transmission
38 coupled to variant emergence and allelic variation. Sci Rep, 2021, 11:7380
- 39 7. Nasir JA, Kozak RA, Aftanas P, Raphenya AR, Smith KM, Maguire F, Maan H, Alruwaili M, Banerjee A,
40 Mbareche H, Alcock BP, Knox NC, Mossman K, Wang B, Hiscox JA, McArthur AG, Mubareka S. A
41 comparison of whole genome sequencing of sars-cov-2 using amplicon-based sequencing, random
42 hexamers, and bait capture. Viruses, 2020, 12
- 43 8. Izquierdo-Lara R, Elsinga G, Heijnen L, Oude Munnink BB, Schapendonk CME, Nieuwenhuijse D, Kon M,
44 Lu L, Aarestrup FM, Lycett S, Medema G, Koopmans MPG, De Graaf M. Monitoring SARS-CoV-2
45 circulation and diversity through community wastewater sequencing, the netherlands and belgium.
46 Emerg Infect Dis, 2021, 27:1405–15
- 47 9. Banada P, Green R, Banik S, Chopoorian A, Streck D, Jones R, Chakravorty S, Alland D. A Simple RT-PCR
48 Melting temperature Assay to Rapidly Screen for Widely Circulating SARS-CoV-2 Variants. MedRxiv
49 Prepr Serv Heal Sci, 2021:2021.03.05.21252709

10. Bonnet G, Tyagi S, Libchaber A, Kramer FR. Thermodynamic basis of the enhanced specificity of structured DNA probes. *Proc Natl Acad Sci U S A*, 1999, 96:6171–6
11. Marras SAE, Kramer FR, Tyagi S. Multiplex detection of single-nucleotide variations using molecular beacons. *Genet. Anal. - Biomol. Eng.*, vol. 14, *Genet Anal*, 1999, pp. 151–6
12. Kostrikis LG, Tyagi S, Mhlanga MM, Ho DD, Kramer FR. Spectral genotyping of human alleles. *Science* (80-), 1998, 279:1228–9
13. Untergasser A, Cutcutache I, Koressaar T, Ye J, Faircloth BC, Remm M, Rozen SG. Primer3-new capabilities and interfaces. *Nucleic Acids Res*, 2012, 40:e115
14. Markham NR, Zuker M. DINAMelt web server for nucleic acid melting prediction. *Nucleic Acids Res*, 2005, 33
15. Tyagi S, Bratu DP, Kramer FR. Multicolor molecular beacons for allele discrimination. *Nat Biotechnol*, 1998, 16:49–53
16. Corman VM, Landt O, Kaiser M, Molenkamp R, Meijer A, Chu DK, Bleicker T, Brünink S, Schneider J, Schmidt ML, Mulders DG, Haagmans BL, Veer B van der, Brink S van den, Wijsman L, Goderski G, Romette J-L, Ellis J, Zambon M, Peiris M, Goossens H, Reusken C, Koopmans MP, Drosten C. Detection of 2019 novel coronavirus (2019-nCoV) by real-time RT-PCR. *Eurosurveillance*, 2020, 25
17. Kim S, Liu Y, Lei Z, Dicker J, Cao Y, Zhang XF, Im W. Differential Interactions Between Human ACE2 and Spike RBD of SARS-CoV-2 Variants of Concern. *BioRxiv*, 2021. <https://doi.org/10.1101/2021.07.23.453598>
18. Khan A, Zia T, Suleman M, Khan T, Ali SS, Abbasi AA, Mohammad A, Wei DQ. Higher infectivity of the SARS-CoV-2 new variants is associated with K417N/T, E484K, and N501Y mutants: An insight from

71 structural data. J Cell Physiol, 2021. <https://doi.org/10.1002/jcp.30367>

72

73

74 **Figures Legends and Table**

Reaction	Oligo	Sequence	Concentration
Tube 1	K417f	5'-GGTGATGAAGTCAGACAAATCG-3'	100 nM
	S.K417N-MB	5'-FAM- <u>ccggcc</u> GCAAACCTGGAAATATTGCTGATTAT ggccgg -BHQ1-3'	250 nM
	S.K417T-MB	5'-Quasar705- <u>ccggct</u> CAAACCTGGAACGATTGCTGAT agccgg -BHQ2-3'	250 nM
	K417r	5'-GCAGCCTGTAAAATCATCTGG-3'	500 nM
	L452Rf	5'-AGGCTGCGTTATAGCTTGGA-3'	100 nM
	S.L452R-MB	5'-Quasar670- <u>cgctcg</u> GGGTAATTATAATTACCGGTATAGATTGTTTAG cgcgacg -BHQ2-3'	250 nM
	L452Rr	5'-TCAGTTGAAATATCTCTCTCAAAGGT-3'	500 nM
	d69-70f	5'-GAACTCAATTACCCCTGCAT-3'	100 nM
	S.d69-70-MB	5'-CFG540- <u>cgctcg</u> GTTCCATGCTAT CTCTGGGACCA cgagcg -BHQ1-3'	150 nM
	d69-70r	5'-TGGTAGGACAGGGTTATCAA-3'	500 nM
	CDC-N1-F	5'-GACCCCAAATCAGCGAAAT-3'	50 nM
	N1-MB	5'-CFR610- <u>cgcgag</u> ACCCCGCATTACGTTTGGTGGACC ctcgcg -BHQ1-3'	50 nM
	CDC-N1-R	5'-TCTGGTACTGCCAGTTGAATCTG-3'	250 nM
	Tube 2	T478Kf	5'-TTGTTTAGGAAGTCTAATCTCAAACC-3'
S.T478K-MB		5'-HEX- <u>ccgcga</u> CCGGTAGCAAACCTTGTAAT tcgcgg -BHQ1-3'	250 nM
S.E484K-MB		5'-CFR610- <u>cgcagg</u> CTTGTAATGGTGTAAAGGTTTTAATTG cctcg -BHQ1-3'	250 nM
S.E484Q-MB		5'-FAM- <u>cgcggg</u> CTTGTAATGGTGTCAAGGTTTTAATTG cccgcg -BHQ1-3'	250 nM
S.N501Y-MB		5'-Quasar670- <u>gCCAAC</u> CCACTTATGGT GTTGGc -BHQ2-3'	250 nM
N501Yr		5'-ACAAACAGTTGCTGGTGCAT-3'	500 nM

75

76 **Table 1.** – Primers and probes used in each assay. Sequences are shown in the 5'→3' direction. Upper case text
77 indicates that it is a binding sequence, underlined text forms the hairpins of the molecular beacons, and bold
78 letters indicate the point mutation nucleotides being identified by that molecular beacon. A gap indicates
79 where the deletion is for the d69-70 molecular beacon. Abbreviations used: CFG = Cal Fluor Gold 540, CFR = Cal
30 Fluor Red 610

31

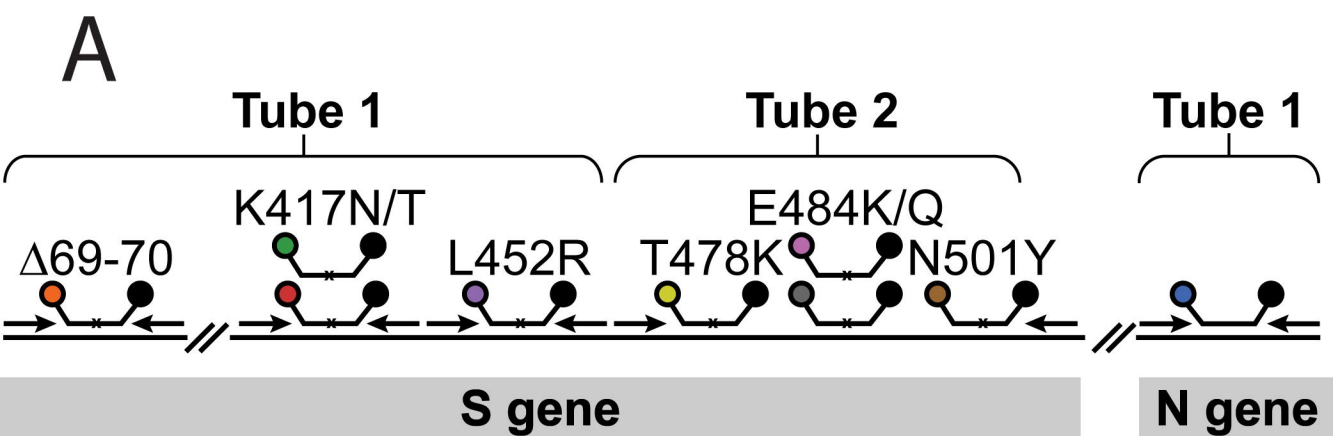
32 **Figure 1. A.** A schematic representation of the primers and molecular beacons used in the assay. A small black
33 **x** on the molecular beacons target binding regions indicates that the molecular beacon is single nucleotide
34 discriminant. **B.** Identifying key mutations present in each variant. The mutations detected in the assay are
35 shown in the rows and variants are shown in the columns. Each of the variants of concern can be identified by
36 these combinations of mutations as well as the variants of interest, see supplemental chart. Abbreviations
37 used: CFG = Cal Fluor Gold 540, CFR =Cal Fluor Red 610, Q670 = Quasar 670, Q705 = Quasar 705.

38
39 **Figure 2.** – The florescence of the T478K discriminating molecular beacon, as a function of temperature, in the
40 presence and absence of targets. When no target is present, dotted line, the fluorescence increases as
41 temperature rises due to the helical order of the stem giving way to a random-coil configuration, separating
42 the fluorophore from the quencher, and resulting in fluorescence. When the molecular beacon binds to its
43 target its stem dissociates which turns on its fluorescence. Due to the increased binding strength of the
44 perfect probe-target hybrid, solid line, compared to the imperfect probe-target hybrid, dashed line, the
45 imperfect-probe target hybrid dissociates at a lower temperature. The PCR monitoring temperature (58°C) is
46 indicated by the vertical dashed line and the window of good discrimination by the shaded area.

47
48 **Figure 3.** – Demonstration of specificity and sensitivity of variant molecular beacon assay. **A.** Each panel shows
49 the amplification curves of a single multiplex reaction using either the Tube one or Tube two specified primers
50 and probes (columns), and the indicated *in vitro* transcribed RNA targets (rows). The ‘wildtype’ template is
51 RNA of the original strain of SARS-CoV-2’s entire genome. The labeled strains contain the RNA sequences of
52 the S gene from the respective SARS-CoV-2 variants and the sample labeled Kappa/Delta uses an RNA
53 corresponding to (positions 1251-1630nt in the Spike protein coding sequence) and containing the E484Q and
54 T478K mutations, which are from the B.1.617 (Kappa) and B.1.617.2 (Delta) variants. This Kappa/Delta Spike

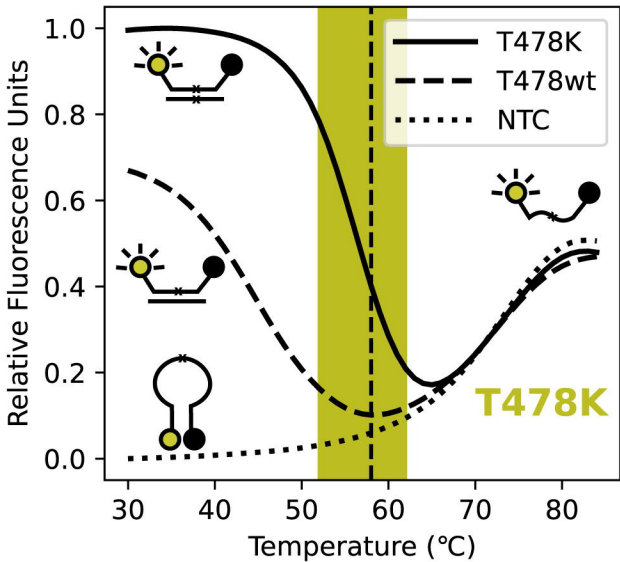
RNA fragment was generated and used due to the lack of commercially available *in vitro* transcribed RNA's at the time. **B.** Sensitivity analysis was run by diluting templates containing the specified mutations from 5,000 copies down to 0.5 copies per reaction. The C_t values are plotted against the template copy number and the correlation coefficients of the natural log of the copy number to the C_t are greater than 0.98 for all amplification products, with around a 3 C_t delay between 10-fold dilutions, both as expected.

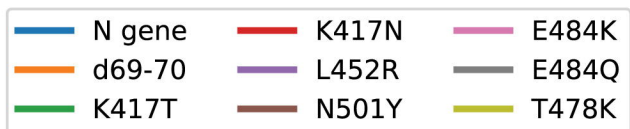
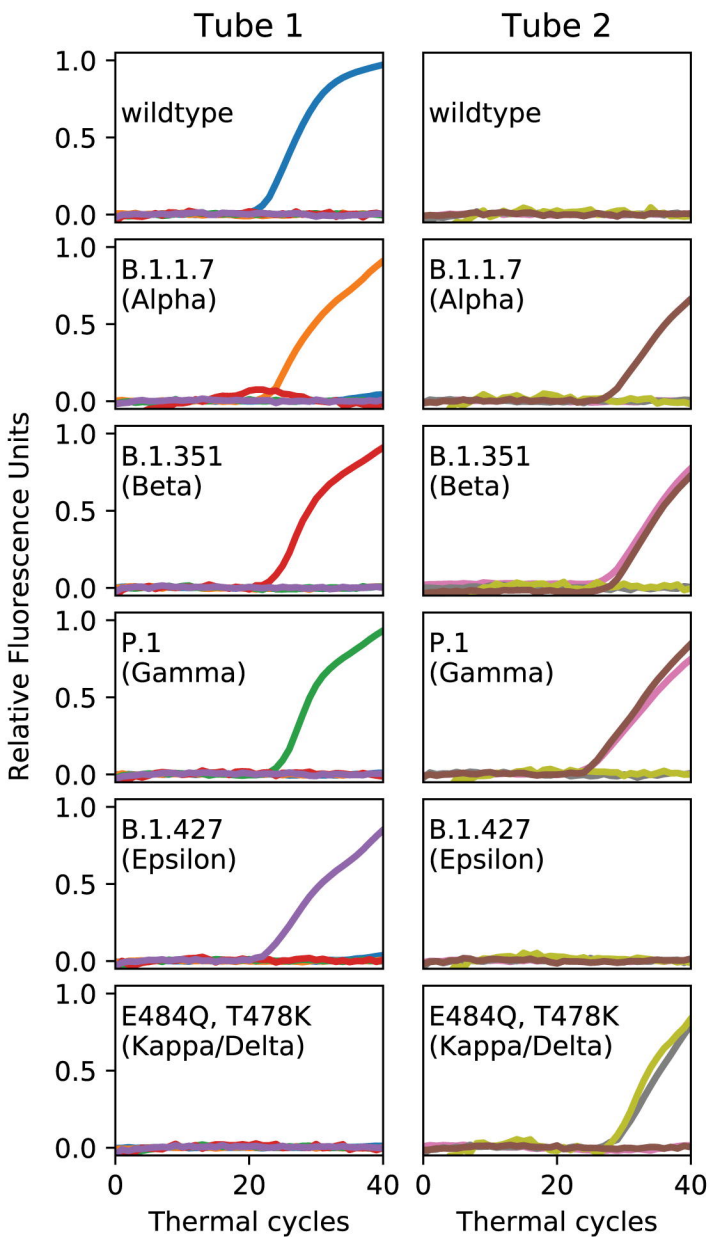
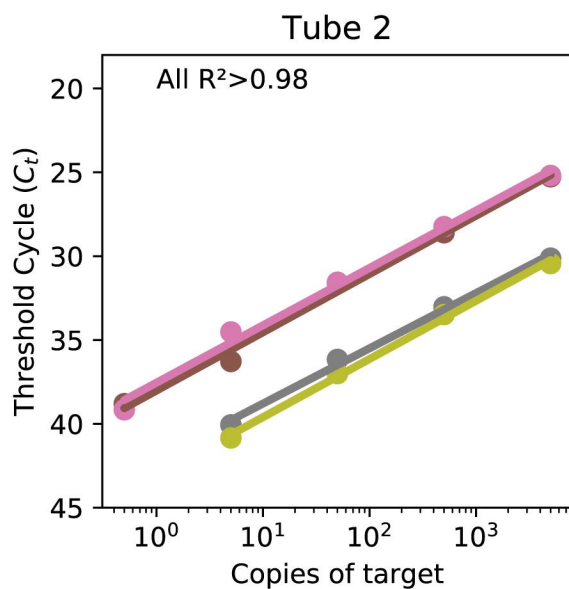
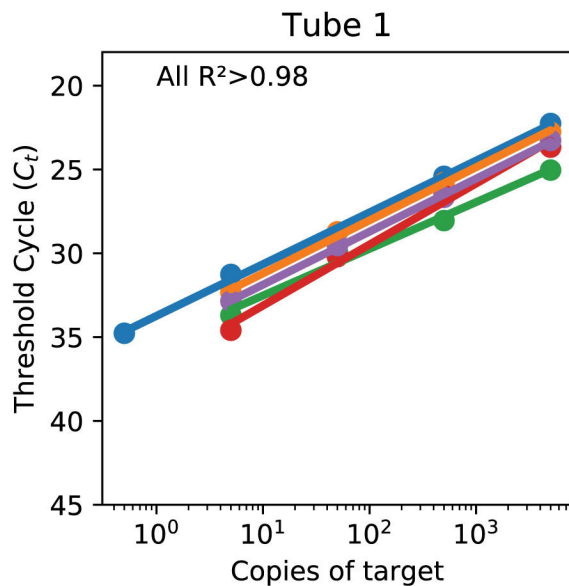
Figure 4. – Threshold cycle (C_t) data for patient samples using our assay. All samples test positive for the N gene control. For the other targets, a C_t value less than 40 indicates the presence of the specified mutation, which can be used to identify the variants of the virus. For example, the presence of the T478K and L452R in pt19 indicates that this virus is the delta variant. All the specified mutations shown in this figure have been sequence confirmed by deep sequencing.



B

		Strain						
	Label	Target	A	VOC B.1.1.7 (Alpha)	VOC B.1.351 (Beta)	VOC P.1 (Gamma)	VOC B.1.617.2 (Delta)	VOI B.1.617.1 (Kappa)
Tube 1	FAM	S.K417N			X			
	CFG	S.d69-70		X				
	CFR	N1	X	X	X	X	X	X
	Q670	S. L452R					X	X
	Q705	S.K417T				X		
Tube 2	FAM	S.E484Q						X
	HEX	S.T478K					X	
	CFR	S.E484K		+/-	X	X		
	Q670	S.N501Y		X	X	X		



A**B**

Threshold Cycles (C_t) of Patient Samples

